Electronic Supplementary Information

Cumulative Enhancement Effect of Proton Conductivity in the Possible Hydrogen Fuel Cell Material Dysprosium Sulfate

Jinxiang Yang,[a] Jiasheng Wang[a], Bo Li*[a], Yuqing Yan*[a],Zhiwu Qiao[a],Haibo Liu[a],Yicong Zhu[a]

[a.] *Hebei Key Laboratory of Hazardous Chemicals Safety and Control Technology, School of Chemical Safety, North China Institute of Science and Technology, Langfang 065201, Hebei, China.*
[*] *Corresponding author.*
E-mail address: libo@ncist.edu.cn, yanyyq80@163.com.

Experimental Details

Synthesis of $\{[(CH_3)_2NH_2]_9Dy_5(SO_4)_{12}\}_n$

Approximately 0.02g of dysprosium chloride hexahydrate ($DyCl_3 \cdot 6H_2O$,0.053mmol) was weighed and added to a glass beaker containing 16 mL of N,N-dimethylformamide (DMF). The solution was transferred to a temperature-controlled magnetic stirrer and completely dissolved. Subsequently, concentrated sulfuric acid (H_2SO_4, 1 mmol) was gradually added to the homogeneous solution. The mixture was maintained under constant magnetic stirring at 100°C for 40 minutes to ensure complete reaction. After allowing the solution to cool naturally to room temperature, it was transferred to a 25 ml Teflon-lined stainless steel autoclave and placed in a forced-air thermostatic drying oven. The reaction was maintained at a constant temperature of 160°C for 24 hours.

After the reaction was completed, the autoclave was allowed to cool slowly to room temperature. The product was washed multiple times with anhydrousethanol. The collected product was placed in a constant-temperature air-blast drying oven and dried at 80°C for 40 minutes. The final product obtained weighed approximately 20 mg (some inevitable loss occurred during transfer of the final product and the washing process). The yield falls within the range of 70% to 80%.

Test of single crystal structure

Intensity data were collected at 120.01(10) K on a four-circle diffractometer using graphite-monochromated Cu Kα radiation (λ = 1.54184 Å). Lorentz and polarization corrections were applied. A multiscan absorption correction was performed using CrysAlisPro 1.171.37.35 (Agilent Technologies) with the SCALE3 ABSPACK scaling algorithm, which employs a spherical harmonics-based empirical correction. The structure was solved by methods with SHELXT-2018 and refined by full-matrix least-squares on F^2 using SHELXL-2018.

Thermogravimetric (TG) analyses of $\{[(CH_3)_2NH_2]_9Dy_5(SO_4)_{12}\}_n$

Thermogravimetric (TG) analyses were performed on an STA-22-0006 thermogravimetric analyzer under nitrogen 10℃ min-1 from 100℃ temperature to 800℃.

Theoretical Calculation Methods

Altering current (AC) impedances were performed for the pellet samples using CorrTest CS chemical Workstation with a conventional two-electrode method; the frequency spans from 1 to 10^6 Hz, and the signal amplitude is 100 mV. The sample was compressed to a pellet under a pressure of 20MPa at room temperature. The pellet was attached to the surface of platinum electrode. The proton conductivity was measured using AC impedance measurement. The thickness of the pellet is 2.02mm. CS sdudio 5 software was used to simulate impedance data to complete the Nyquist plot and obtain the resistance value. The proton conductivity (σ, S cm^{-1}) of the sample was estimated by using theequation:

$\sigma = L/RS$

where L is the thickness, S is the area of the measured plate; R is the measured impedance. The activation energy (E_a) is calculated by using the conductivity data between 100 and 250℃ with the Arrhenius equation:

$Ln(\sigma T)=lnA-E_a/k_BT$

where k_B and A are the Boltzmann constant and the pre-exponential factor, respectively.

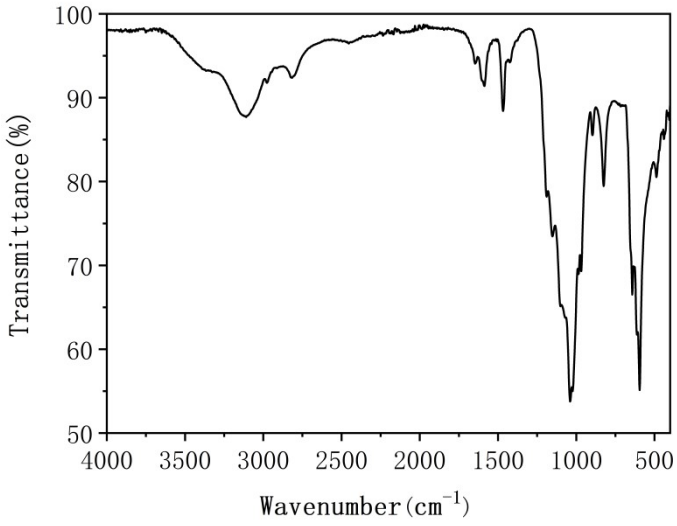

Fig.S1 The IR spectra of $\{[(CH_3)_2NH_2]_9Dy_5(SO_4)_{12}\}_n$.

In the infrared (IR) spectrum of $\{[(CH_3)_2NH_2]_9Dy_5(SO_4)_{12}\}_n$ (Fig.S1), two absorption peaks in the range of 3500–3000 cm^{-1} and a peak at 1600 cm^{-1} are attributed to the characteristic stretching and bending vibrations of N–H bonds, respectively. The

absorption peak at 2850 cm^{-1} corresponds to the C–H stretching vibrations of methyl groups, while the asymmetric bending vibration of methyl groups is observed at 1460 cm^{-1}. The presence of both N–H and methyl groups confirms the existence of dimethylammonium cations within the pores. Additionally, three characteristic absorption peaks at 1120 cm^{-1}, 990 cm^{-1}, and 610 cm^{-1} are assigned to the vibrational modes of sulfate groups, verifying their successful coordination to the metal center. The combined IR spectral analysis demonstrates the successful coordination of sulfate groups and the presence of dimethylammonium cations in the pore channels of the coordination polymer, thereby confirming the successful synthesis of complex .

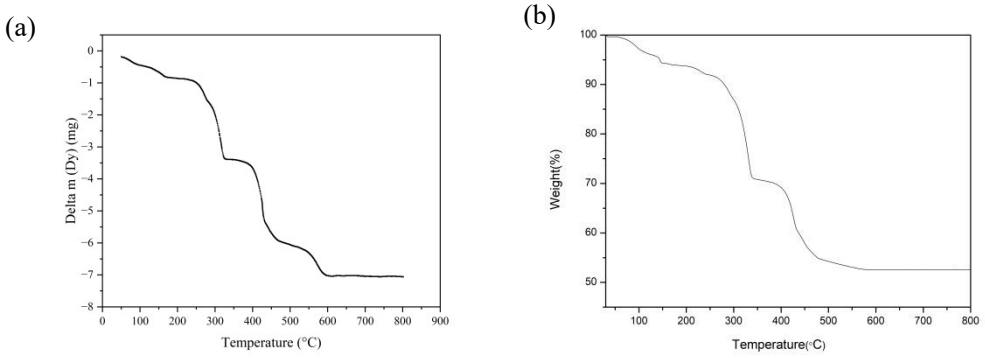

Fig.S2 (a) The thermogravimetric curves of $\{[(CH_3)_2NH_2]_9Dy_5(SO_4)_{12}\}_n$ before cycling tests under a nitrogen atmosphere. (b) The thermogravimetric curves of $\{[(CH_3)_2NH_2]_9Dy_5(SO_4)_{12}\}_n$ after cycling tests under a nitrogen atmosphere.

The thermogravimetric analysis of $\{[(CH_3)_2NH_2]_9Dy_5(SO_4)_{12}\}_n$ revealed distinct mass lo ss stages across the temperature range of 50–800 °C. As illustrated in the TG curve (Fig. 2b), a minor initial mass loss occurred between 50–150 °C, likely due to the release of tr ace adsorbed water from the material surface under ambient conditions. A stable plateau was observed between 150–250 °C, indicating no significant structural degradation within t his temperature regime. Above 250 °C, the decomposition process commenced, marked by two sequential stages:

First decomposition step (250°C–400°C): Corresponding to the loss of dimethylammon ium cations residing within the framework channels.

Second continuous mass loss (>400 °C): Attributable to the gradual collapse of the cr ystalline framework, as corroborated by complementary structural analyses.

Notably, the absence of mass loss or structural changes below 250 °C underscores th e exceptional thermal stability of {[(CH3)2NH2]9Dy5(SO4)12}n under anhydrous high-tem perature conditions. Fig.S2a and 2b reveal that the framework of the complex remains inta ct after cycling tests, confirming no significant structural degradation.

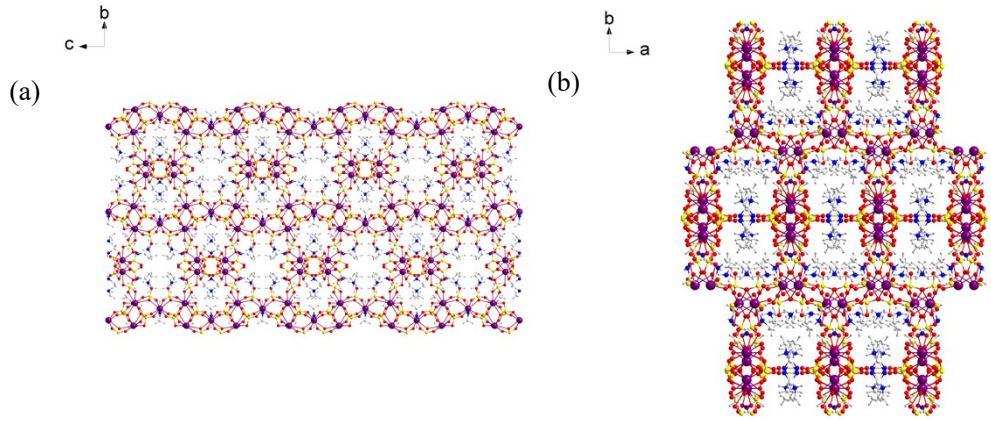

Fig.S3 (a) Crystal packing of $\{[(CH_3)_2NH_2]_9Dy_5(SO_4)_{12}\}_n$ along the a-axis, showing full cationic comp onents. (b) Crystal packing of $\{[(CH_3)_2NH_2]_9Dy_5(SO_4)_{12}\}_n$ along the c-axis, showing full cationic componen ts.(Purple: Dy atoms; Yellow: S atoms; Red: O atoms; Blue: N atoms; Gray: C atoms; White: H atoms;)

The combined IR spectral (Fig.S1) and Fig.S3 analysis demonstrates the successful coordination of sulfate groups and the presence of dimethylammonium cations in the pore channels of the coordination polymer, thereby confirming the successful synthesis of complex .

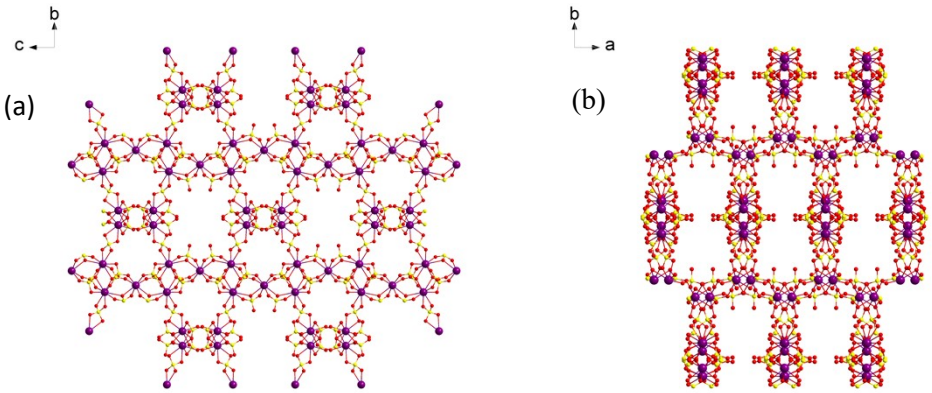

Fig.S4 (a) Cation-free view of crystal packing in $\{[(CH_3)_2NH_2]_9Dy_5(SO_4)_{12}\}_n$ along a-axis. (b) Cation-free view of crystal packing in $\{[(CH_3)_2NH_2]_9Dy_5(SO_4)_{12}\}_n$ along c-axis. (Purple: Dy atoms; Yellow: S atoms; Red: O atoms;)

Table S1 Main crystallographic parameters

formula	$\{[(CH_3)_2NH_2]_9Dy_5(SO_4)_{12}\}_n$		
weight(g/mol)	2387.02	*c* (Å)	18.5109(3)
shape	Block	α (º)	90
color	White	*β* (º)	94.1021(15)
T (K)	120.01(10)	γ(º)	90
crystal system	monoclinic	*V* (Å3)	6425.76(18)
space group	*C2/c*	*Z*	4
a (Å)	10.03321(16)	*F* (000)	4596
b (Å)	34.6874(6)	*R*int	3.32%

Table S2 Hydrogen Bonds

D	H	A	d(D-H)/Å	d(H-A)/Å	d(D-A)/Å	D-H-A/°
N015	H01A	O17	0.89	2.12	2.888(9)	144.0
N016	H016	O2[1]	0.86	2.10	2.890(10)	153.2
N1	H1A	O23	0.89	1.99	2.830(6)	156.1
N1	H1B	O24[2]	0.89	2.00	2.881(6)	172.3

Table S3 Electrical conductivity of lanthanide-containing materials

Composition	Condition	Conductivity(S/cm)
$BaCe_{0.9}Y_{0.1}O_{2.95}$	800 °C,5%H2–95%Ar	9.20×10^{-3}
$CaZr_{0.95}Yb_{0.5}O_3$-delta	899.85°C,hydrogen andoxygen atmosphere	1.28×10^{-3}
$Na_4Y_{0.6}P_{0.2}Si_{2.8}O_9$	300°C	3.8×10^{-4}
$Gd_{2.9}Sr_{0.1}GaO_{5.95}$	600°C,wet Ar atmosphere	1×10^{-3}
$La_{0.2}Nd_{0.2}Sm_{0.2}Gd_{0.2}Eu_{0.2}NbO_4$	800°C,wet atmosphere	3.0×10^{-6}

[1]Y. P. Fu and C. S. Weng, Ceram. Int., 2014, **40**, 10793-10802.

[2]C. G. Lei，F. L. Zhang and X. Wu, Ionics, 2024, **30**, 2715-2727.

[3]T. Okura, N. Matsuoka Y. Takahashi, N. Yoshida and K. Yamashita, Materials, 2023, **16**, 2155.

[4]A. Iakovleva, A. Chesnaud, I. Animitsa and G. Dezanneau, Int. J. Hydrogen Energy., 2016, **41**, 14941-14951.

[5]A. A. A. Elameen, A. Dawczak, T. Miruszewski, M. Gazda and S. Wachowski, PCCP, 2023, **25**, 8.